Development and Validation of a Water-to-Air Heat Pump Model Using Modelica

Yuhang Zhang[1] Mingzhe Liu[1] Zhiyao Yang[1] Caleb Calfa[1] Zheng O'Neill[1]

[1]J Mike Walker' 66 Department of Mechanical Engineering, Texas A&M University, USA,
{yuhang.zhang,mingzhe.liu,z.yang,cjcalfa,zoneill}@tamu.edu

Abstract

Water-to-air heat pumps are widely used Heating, Ventilation, and Air Conditioning (HVAC) devices due to their versatility and energy efficiency. However, there is a scarcity of readily available Modelica models that support reversible operation (heating and cooling modes), use compressor speed as the control signal, and accurately predict the system performance. To address this gap, this paper presents a speed-input water-to-air heat pump model developed using Modelica. Performance curves are employed to represent the functionality and predict the system's capacity and power usage. To validate the proposed model's effectiveness, manufacturer-provided data are used to generate the performance curves. The model, based on these curves, is then used to simulate testing conditions, which are implemented in a real heat pump testbed. The comparison between simulated and measured values shows that the errors during normal operation stages are within an acceptable range, demonstrating the effectiveness of the developed water-to-air heat pump model.

Keywords: Modelica, Water-to-air heat pump, Performance curve, Validation

1 Introduction

Water-to-air heat pumps are versatile HVAC devices capable of providing both heating and cooling by transferring heat between water and air. They have gained wide applications due to their energy efficiency, ability to reduce operating costs, and environmentally friendly characteristics. Unlike air-source heat pumps (ASHP) which exchange heat from the outside air, water source heat pumps (WSHP) use water as its heat source or heat sink to provide heating or cooling. The water source could be a lake, river, pond, groundwater, or a closed-loop system where water circulates through buried pipes. Because water has a higher heat capacity and generally maintains more stable and moderate temperatures compared to air, WSHPs tend to be more energy-efficient and weather-independent. In addition, WSHPs are favored for their quiet operation and long lifespan (Chua, Chou, and Yang 2010; Gaur, Fitiwi, and Curtis 2021). These characteristics make WSHPs become a good choice for both residential and commercial buildings, especially where a reliable water source is available or where ground temperatures are stable.

In particular, heat pump-based heating and cooling systems are increasingly being integrated into building-to-grid systems for electrifications. This integration allows buildings equipped with these heat pumps to participate in demand response programs, where the operation of the HVAC system can be adjusted based on the needs of the grid. During periods of peak demand, the heat pumps can reduce their load or shift their operation to off-peak hours, contributing to grid stability and enabling a better use of renewable energy sources. This capability not only provides economic benefits to building owners through incentives and reduced energy bills, but also supports the broader goal of creating a more resilient and sustainable energy infrastructure.

As modeling is a widely acknowledged tool for better understanding, analyzing, and applying heat pumps, numerous studies have been conducted on the development and improvement of heat pump models for various applications (Montagud, Corberán, and Ruiz-Calvo 2013; Baccoli, Mastino, and Rodriguez 2015; Huang et al. 2019). Among these, Modelica, an object-oriented, equation-based language, has been widely adopted in the modeling of heat pumps due to its ability to directly incorporate physical laws into models, facilitate reusable components, and support multi-domain simulations (Fritzson and Engelson 1998). For example, the Modelica Buildings library's Buildings.Fluid.HeatPumps.EquationFitReversible is built upon the curves-based model from EnergyPlus (Crawley et al. 2001) and mainly used for water to water heat pump; the control input of this model is the set point for the leaving fluid temperature (Wetter et al. 2014). The IDEAS library (Jorissen et al. 2018) developed by KU Leuven and 3E offers models of air-to-air and water-to-water heat pumps, but none of aforementioned heat pump models incorporate the compressor speed as a control variable for the heat pump with variable speed drivers, while it is anticipated that inverter-based heat pump will play more roles for electrifying buildings. Additionally, the AixLib (Maier et al. 2024) developed a generic grey-box heat pump model (`AixLib.Fluid.HeatPumps.HeatPump`) that employs empirical data for modeling the refrigerant cycle. This model enables the heat pump on/off control and inverter based reversible operation. However, this model lacks support for water-to-air heat pump applications. The DLR ThermoFluid Stream Library (Zimmer, Meißner, and Weber 2022) provides robust modeling of complex thermofluid architectures including heat pumps. However, it focuses more on detailed vapor compression component modeling, which can be computationally inefficient for overall system performance. Moreover, this model has not yet been validated.

To the best of the authors' knowledge, there is no readily available and open-source variable-speed water-to-air heat pump model in Modelica that simultaneously meets the following requirements: 1) utilizes the compressor speed as a control signal, 2) seamlessly switches between heating and cooling modes, 3) predicts power usage and capacity, including both sensible and latent components. 4) has been validated using experiment measurements.

The development of such a model is crucial. Since the performance of variable-speed heat pump systems is directly influenced by compressor speed, this model enables more accurate simulations to predict overall system performance, including power usage and both sensible and latent heat capacity under various speed conditions. This is particularly important for control applications, where utilizing compressor speed as a control variable provides a more direct method of adjusting system performance. Modulating compressor speed directly affects the system's capacity and energy consumption, allowing for more precise management of the heat pump's operation. By incorporating compressor speed into the model, engineers can develop and test advanced control strategies that dynamically respond to changing conditions, thereby improving system efficiency and occupant comfort.

The lack of such a model also limits the ability to fully explore building-to-grid integration. A model with compressor speed control could be used to simulate the heat pump's behavior in response to grid signals, helping to design systems that can participate in demand response programs and contribute to grid stability. This integration is a key component of creating energy-efficient buildings that can interact seamlessly with the broader energy grid. In summary, developing a reversible water-to-air heat pump model that takes the compressor speed as a control signal in Modelica is not only necessary for improving the performance and efficiency of HVAC systems but also for advancing research in building energy management and grid integration. Therefore, in this study, a variable-speed reversible water-to-air heat pump model developed using Modelica is presented. The developed water-to-air heat pump model is based on the performance curve method and is capable of supporting the reversible operation (i.e., heating and cooling modes), taking the compressor speed as the control signal to facilitate the investigation of advanced control methods.

The paper is organized as follows: Section 2 introduces the model development process, beginning with a concise introduction to the major components and working principles of water-to-air heat pumps. It then details the Modelica implementation, including interfaces and performance curves. In Section 3, the validation process is described, where simulation results using the developed Modelica model are compared with measurements from a real heat pump testbed. In Section 4, the applicability of the developed model across various heat pump operating stages is discussed. Finally, Section 5 concludes this study.

2 Modelica Development

2.1 Overview of Water-to-Air Heat Pumps

A typical water-to-air heat pump consists of several key components: a compressor, an expansion valve, two heat exchangers (a refrigerant-to-water heat exchanger and a refrigerant-to-air heat exchanger), and a reversing valve. Among these, the compressor, expansion valve, and the two refrigerant heat exchangers are the primary components of the refrigeration cycle, which provides the essential functions of heating and cooling. The reversing valve, located between the compressor and the refrigerant-to-water heat exchanger, enables the reversal of refrigerant flow, allowing the system to switch between heating and cooling modes. Figure 1 illustrates the schematic of the heat pump's heating and cooling cycles. In heating mode, the heat pump extracts heat from the water side (acting as the evaporator) and releases heat into the air side (acting as the condenser), resulting in an increase in room temperature. Conversely, in cooling mode, the reversing valve reverses the refrigerant flow, causing the water side to function as the condenser and the air side to function as the evaporator. Heat is then transferred from the indoor air to the refrigerant, thereby lowering the indoor air temperature.

2.2 Modelica Implementation

Despite including all the aforementioned components in the water-to-air heat pump, the focus of this study is to predict the overall heat pump performance rather than the performance of individual components. Therefore, a vapor compression cycle with each component was not modeled. Instead, performance curves are used to represent the functionality of water-to-air heat pumps due to their

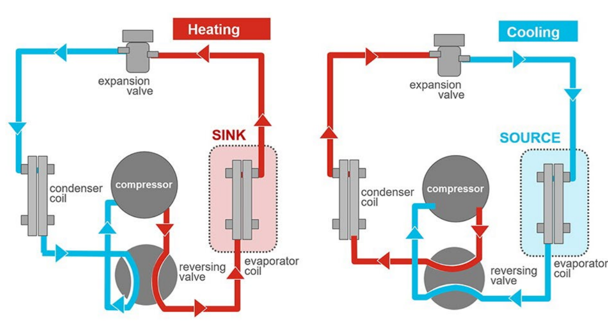

Figure 1. Schematic of the heating and cooling cycles in a reversible water-to-air heat pump (Trane Technologies 2024a)

simplicity in implementation and wide application (Ying Zhang et al. 2020).

The proposed model was developed based on the following assumptions:

1. The model uses heating/cooling/off signals and the compressor speed as control inputs.

2. The steady-state performance of the heat pump, including total capacity ($\dot{Q}$) and Energy Input Ratio (EIR), is computed using polynomial equations. These equations account for the mass flow fractions on both the water and air sides, the inlet temperatures on both sides, and the compressor speed ratio.

Figure 2 shows the Modelica diagram of the developed heat pump model. To simplify and expedite the modeling process, DX coil models (`Buildings.Fluid.DXSystems`) from the Modelica Buildings Library (version 10.0.0) are reused and modified to develop the heat pump model in this study. (Wetter et al. 2014). Two data records (`datCoiHea` and `datCoiCoo`) are included in the model to record the nominal values and performance curves for heating mode and cooling mode, respectively.

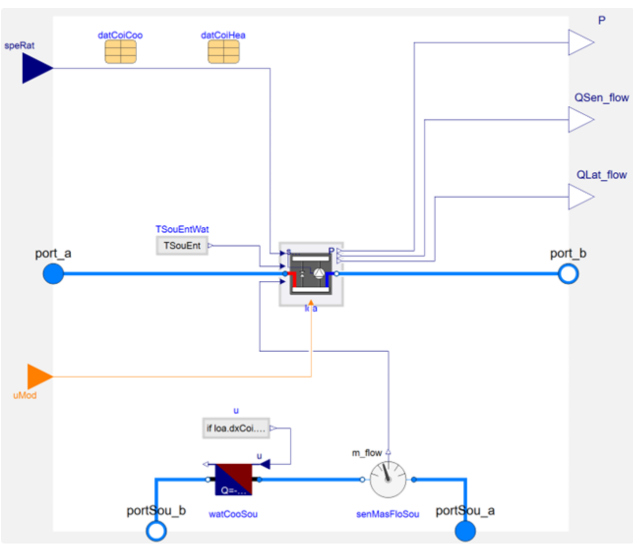

Figure 2. Diagram of the heat pump model in Dymola.

Table 1 lists all the connectors of the developed heat pump model. The model inputs include system operating mode (`uMod`), compressor speed (`speRat`). Both waterside and airside inlet information, such as flow rates, temperatures, and humidity ratios, are read from fluid ports. The model then calculates the real-time system capacity and power usage based on this information. These outputs can also be read from the interfaces shown in Figure 2.

The proposed model calculates the steady-state total capacity ($\dot{Q}$) and energy input ratio (EIR) at off-designed conditions based on Equation 1 and Equation 2, respectively. Both these equations are the product of functions

Table 1. Connectors of the developed heat pump model.

Type	*Name*	*Description*
FluidPort_a	`port_a`	Fluid connector for the inlet of the load side
FluidPort_b	`port_b`	Fluid connector for the outlet of the load side
FluidPort_a	`portSou_a`	Fluid connector for the inlet of the source side
FluidPort_b	`portSou_b`	Fluid connector for the outlet of the source side
input RealInput	`speRat`	Speed ratio [1]
input IntegerInput	`uMod`	Controlinput signal, cooling mode=-1, off=0, heating mode=+1
output RealOutput	`P`	Electrical power consumed by the unit [W]
output RealOutput	`QSen_flow`	Sensible heat flow rate of the load side [W]
output RealOutput	`QLat_flow`	Latent heat flow rate of the load side [W]

that account for changes in the inlet temperatures of both the source side (waterside) ($\theta_{\mathrm{loa,in}}$) and load side (airside) ($\theta_{\mathrm{sou,in}}$), changes in mass flow rates of both the source side ($\dot{m}_{\mathrm{sou}}$) and load side ($\dot{m}_{\mathrm{loa}}$) and compressor speed ratio (*speRat*).

$$\dot{Q}\left(\theta_{loa,in}, \theta_{sou,in}, ff_{loa}, ff_{sou}\right) = cap_{\theta}\left(\theta_{loa,in}, \theta_{sou,in}\right) \times cap_{FFLoa}\left(ff_{loa}\right) \times cap_{FFSou}\left(ff_{sou}\right) \times cap_{spe}\left(speRat\right) \times \dot{Q} \tag{1}$$

$$EIR\left(\theta_{loa,in}, \theta_{sou,in}, ff_{loa}, ff_{sou}\right) = EIR_{\theta}\left(\theta_{loa,in}, \theta_{sou,in}\right) \times EIR_{FFLoa}\left(ff_{loa}\right) \times EIR_{spe}\left(speRat\right) / COP_{nom} \tag{2}$$

where $\theta_{loa,in}$ is the inlet temperature of the load side (airside), which is the dry-bulb air temperature if the coil is dry or the wet-bulb air temperature if the coil is wet. $\theta_{sou,in}$ is the inlet temperature of the source side (waterside). ff_{loa} is the normalized mass flow rate at the load side and is calculated as $\dot{m}_{loa}/\dot{m}_{loa,nom}$. ff_{sou} is the normalized mass flow rate at the source side and is calculated as $\dot{m}_{sou}/\dot{m}_{sou,nom}$. $\dot{m}_{loa,nom}$ is the nominal mass flow rate at the load side, and $\dot{m}_{sou,nom}$ is the nominal mass flow rate at the source side. The capacity modifiers cap_{θ}, cap_{FFLoa}, cap_{FFSou}, cap_{spe} and the EIR modifiers EIR_{θ}, EIR_{FFLoa}, EIR_{FFSou}, EIR_{spe} are functions of inlet temperatures, load side flow rate, source side flow rate, and compressor speed ratio, respectively. These modifiers can be calculated using Equation 3 to Equation 10:

$$cap_{\theta}(\theta_{loa,in}, \theta_{sou,in}) = a_1 + a_2\theta_{loa,in} + a_3\theta_{loa,in}^2 + a_4\theta_{sou,in} + a_5\theta_{sou,in}^2 + a_6\theta_{loa,in}\theta_{sou,in} \quad (3)$$

$$cap_{FFLoa}(ff_{loa}) = b_1 + b_2ff_{loa} + b_3ff_{loa}^2 + b_4ff_{loa}^3 + \ldots \quad (4)$$

$$cap_{FFSou}(ff_{sou}) = c_1 + c_2ff_{sou} + c_3ff_{sou}^2 + c_4ff_{sou}^3 + \ldots \quad (5)$$

$$cap_{spe}(speRat) = d_1 + d_2speRat + d_3speRat^2 + \ldots \quad (6)$$

$$EIR_{\theta}(\theta_{e,in}, \theta_{c,in}) = e_1 + e_2\theta_{loa,in} + e_3\theta_{loa,in}^2 + e_4\theta_{sou,in} + e_5\theta_{sou,in}^2 + e_6\theta_{loa,in}\theta_{sou,in} \quad (7)$$

$$EIR_{FFLoa}(ff_{loa}) = f_1 + f_2ff_{loa} + f_3ff_{loa}^2 + f_4ff_{loa}^3 + \ldots \quad (8)$$

$$EIR_{FFSou}(ff_{sou}) = g_1 + g_2ff_{sou} + g_3ff_{sou}^2 + g_4ff_{sou}^3 + \ldots \quad (9)$$

$$EIR_{spe}(speRat) = h_1 + h_2speRat + h_3speRat^2 + \ldots \quad (10)$$

The coefficients used in the above performance curves can be obtained by fitting the performance data provided by manufacturers or from on-site measurements. It should be noted that although the form of the performance curves is identical for heating and cooling operation modes, different coefficients should be used and fitted respectively.

3 Validation

3.1 Heat Pump Testbed

To validate the effectiveness of the developed heat pump model, measurement data were gathered from an actual heat pump testbed situated at Texas A&M University and then compared with the simulated values using the proposed heat pump model.

Figure 3 shows a photograph of the heat pump testbed. The heat pump used in the testbed is a 2-ton water-to-air heat pump. Load emulators are equipped within the testbed to emulate various testing conditions. Multiple sensors are installed to collect and monitor real-time inlet and outlet conditions for both the waterside and airside, compressor speed, and unit power consumption. A more detailed introduction to the testbed can be found in (Calfa et al. 2023). Table 2 shows part of the rated information from the product catalog (Trane Technologies 2024b).

Table 2. Rated information of the studied heat pump model.

Parameter	*Value*
Water side flow rate [kg/s]	0.39
Air side flow rate [m3/s]	0.44
Cooling capacity [kW]	7.21
Cooling COP [-]	5.4
Heating capacity [kW]	8.88
Heating COP [-]	6.1

3.2 Performance Curves from Manufacturer Datasets

The performance curves of the heat pump model are fitted using the dataset provided by the manufacturer, which includes various inlet conditions for both the waterside and airside. The range of each normalized dependent variable in the performance curves is shown in Table 3.

Table 3. Rated information of the studied heat pump model.

Variable	*Range*
Normalized water flow rate [-]	[0.65, 1]
Normalized air flow rate [-]	[0.46, 1]
Air inlet dry bulb temperature [°C]	[21.1, 32.2]
Air inlet wet bulb temperature [°C]	[11.3, 23.8]
Water inlet temperature [°C]	[7.2, 35]
Compressor speed ratio [-]	[0.5, 1]

The data sets are divided into two distinct subsets: training and test sets, with an 80:20 split ratio. The curve fitting process utilizes solely the data from the training set. The generalized least squares method is used to estimate the coefficients for the performance curves, as introduced in Section 2. Table 4 lists part of the estimated coefficients of performance curves as examples.

Following the training process, the fitted performance curves are tested on the test set to evaluate the fitting accuracy. Figure 4 presents the model performance for cooling and heating operations using the test set. The results indicate that the overall fitting of the heat pump's performance is satisfactory for both heating and cooling conditions, with most prediction errors falling within 15%. To further quantitatively evaluate the model performance, Normalized Mean Bias Error (NMBE) and Coefficient of Variation of the Root Mean Squared Error (CVRMSE) are used as performance metrics to reflect the error between the simulated and measured values. The equations to calculate NMBE and CVRMSE are shown in Equation 11 and Equation 12, respectively.

$$\text{NMBE} = \frac{\sum_{i=1}^{n}(y_i - \hat{y}_i)}{n \times \bar{y}} \times 100\% \quad (11)$$

$$\text{CVRMSE} = \frac{\sqrt{\frac{1}{n}\sum_{i=1}^{n}(y_i - \hat{y}_i)^2}}{\bar{y}} \times 100\% \quad (12)$$

where y_i are the observed values, $\hat{y}_i$ are the predicted values, $\bar{y}$ is the mean of observed values, and n is the number of observations.

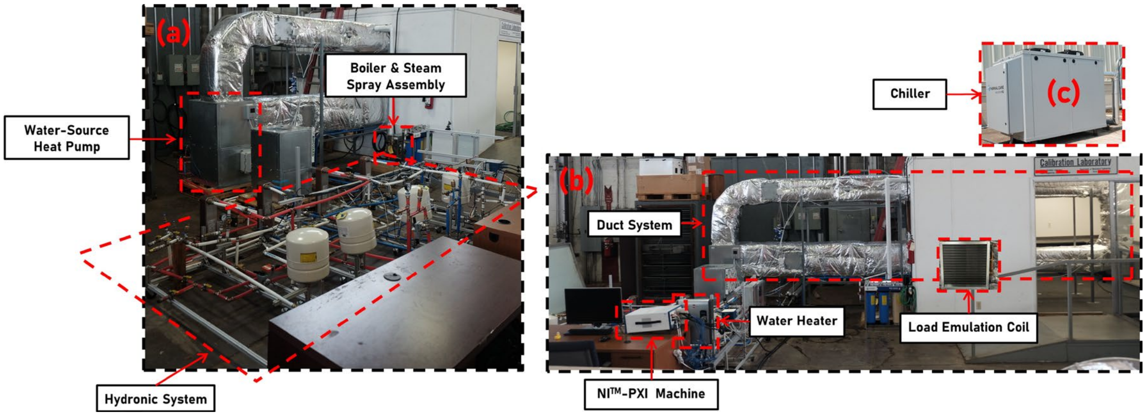

Figure 3. A photograph of the heat pump testbed (Calfa et al. 2023)

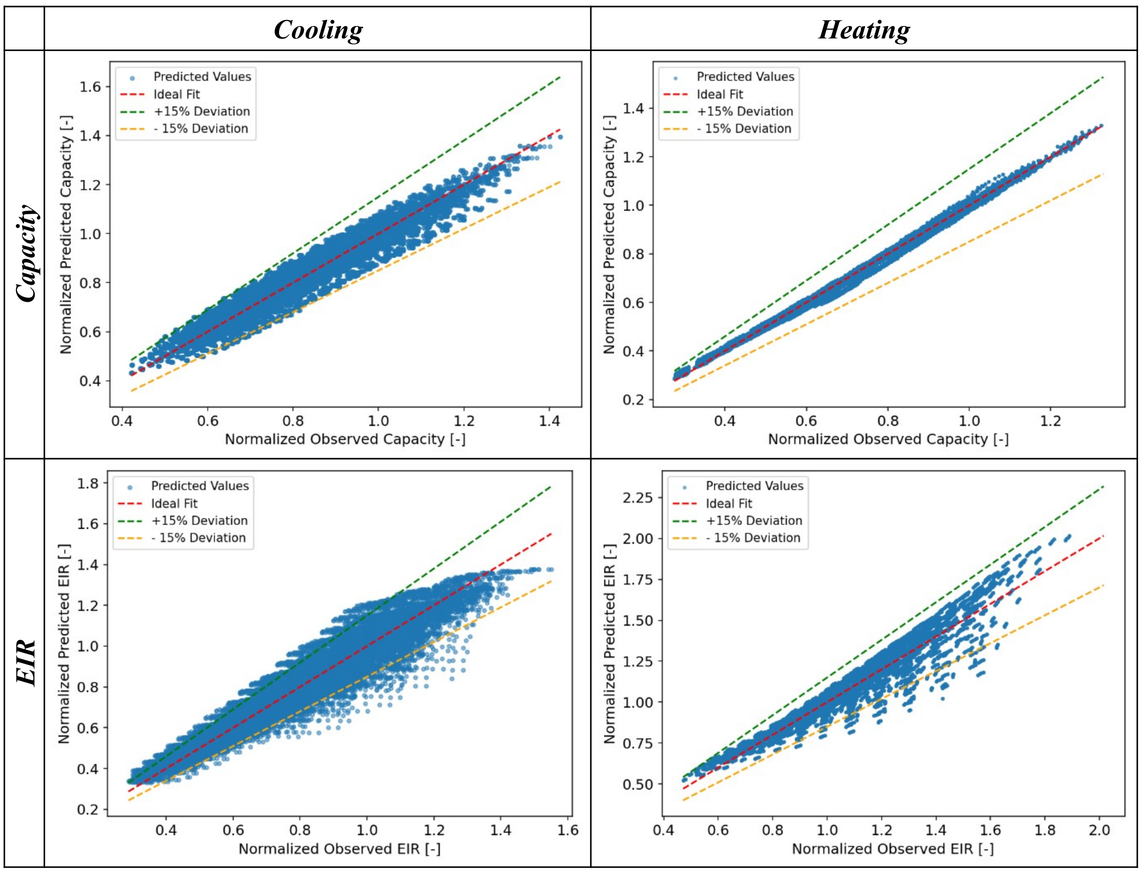

Figure 4. Prediction performance of WSHP performance curve on the testing dataset.

Table 4. Estimated coefficients of performance curves.

Performance curve	*Cooling*	*Heating*
$cap_{\theta}(\theta_{loa,in}, \theta_{sou,in})$	[0.4861, 0.03002, -2.128×10^{-4},-1.376×10^{-4}, -2.067×10^{-5}, -1.994×10^{-4}]	[0.4593, -0.0013051, -1.902×10^{-5}, 0.01901, 4.276×10^{-5}, -1.448×10^{-4}]
$cap_{FFLoa}(ff_{loa})$	[0.7686, 0.315]	[0.8935, 0.1463]
$cap_{FFSou}(ff_{sou})$	[0.9856, 0.01642]	[0.9213, 0.07482]
$cap_{spe}(speRat)$	[0, 1.628, -0.4200]	[0, 1.807, -0.1575]

Table 5 presents the performance metrics on the test set, demonstrating the accuracy of the predictive model. This model will then be applied to the actual measurement dataset for additional validation.

Table 5. Performance metrics on the test set.

	NMBE Cooling	*CVRMSE Cooling*	*NMBE Heating*	*CVRMSE Heating*
Capacity	0.039%	5.70%	0.159%	2.23%
EIR	0.121%	8.19%	0.039%	7.47%

3.3 Validation with Experimental Datasets

Various testing conditions are conducted in the testbed, and data are collected accordingly. After data preprocessing, such as excluding data points recorded during startup/shutdown cycles, a total of 311 data points are obtained for cooling mode and 181 data points are obtained for heating mode. Figure 5 uses compressor speed as an example to illustrate the data distribution for both manufacturer and measurement data. For each data point, the monitored conditions as listed in Table 1 are used as inputs for the developed Modelica heat pump model. After the simulations, the model outputs are compared with the measurements. The compared values include heating/cooling capacity, EIR and electricity power. Figure 6 shows comparisons between simulated and measured values for capacity, EIR, and power in cooling and heating modes, respectively. Table 6 presents the calculated performance metrics.

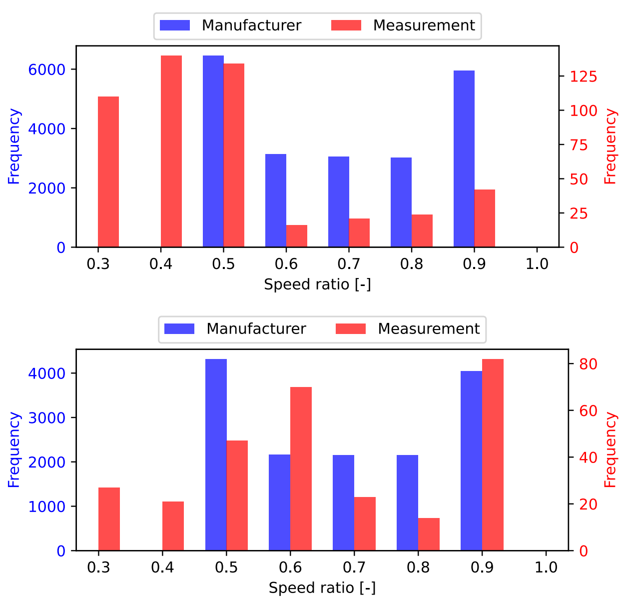

Figure 5. Data distribution of compressor speed ratio for both manufacturer and measurement data in cooling (top) and heating (bottom) modes.

Table 6. Performance metrics on the measurement set.

	NMBE Cooling	*CVRMSE Cooling*	*NMBE Heating*	*CVRMSE Heating*
Capacity	1.09%	3.77%	4.89%	8.22%
EIR	1.24%	-5.33%	3.96%	9.77%
Power	2.96%	-1.32%	5.67%	5.85%

From the comparison results, it can be observed that the simulated values using the developed model generally align with the observed values, and the error metrics are within an acceptable range, validating the effectiveness of the developed reversible water-to-air heat pump model. The discrepancy between the simulated and measured values might arise from the following sources:

1. Model Simplifications and Assumptions: The proposed heat pump model uses simplified performance curves to represent its performance. Although the results prove its effectiveness, some inevitable model errors arise from this simplification.

2. Measurement Errors: Due to sensor uncertainties, measurement values can have errors, leading to discrepancies. This error can be mitigated by using highly accurate sensors.

4 Discussions

This section evaluates the effectiveness of the developed WSHP model by comparing continuous testing conditions gathered from two full days of operation—one focused on cooling and the other on heating. Unlike the validation section which only considers normal steady-state running stages, the testing conditions here encompass all heat pump operation stages, including startup, normal steady-state running, and shutdown phases. Data were sampled at 5-second intervals, with a rolling average applied—5 minutes for the heating day and 3 minutes for the cooling day—resulting in 288 testing points for cooling and 480 for heating. The model required inputs detailed in Table 1 are obtained from onsite measurements and then fed into the developed model. The simulation outputs are subsequently compared with the measured values, specifically focusing on system capacity as a comparison example. Figure 7 presents the comparison results for two days with cooling and heating operations, respectively. The figure uses a yellow background to denote continuous steady-state operation stages and a pink background to highlight other stages, including startup, shutdown cycles, and off periods.

From Figure 7, it can be observed that during normal steady-state operation periods, the predicted system capacity closely matches the measured values. However, during startup and shutdown cycles, the model fails to capture the transient variations for the system capacity, leading to discrepancies between the predicted and measured

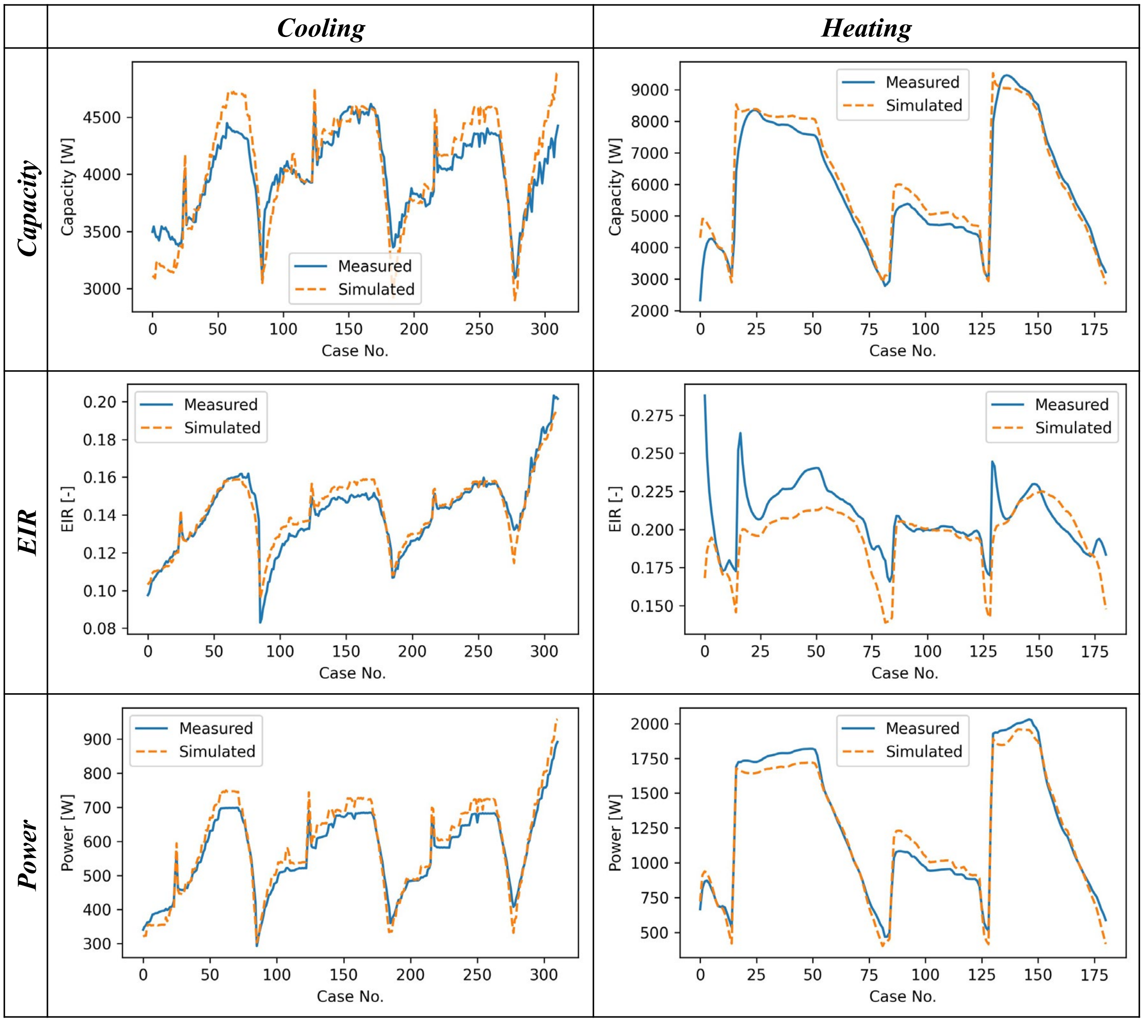

Figure 6. Comparison between simulated and measured values for system capacity, EIR, and power.

values. The comparison results demonstrate the application restrictions of the proposed heat pump model. As the performance curves adopted in the proposed model are only valid during stable operation conditions, this model is not suitable for simulating transient heat pump performance, such as startup and shutdown cycles. Therefore, other modeling approaches should be considered if transient behaviors are expected. In particular, behaviors from Pulse Width Modulation (PWM) to adjust the system capacity need to be incorporated.

5 Conclusions and Future Work

In this paper, a new inverter-based variable-speed water-to-air heat pump model developed in Modelica is presented. This model is expanded and modified based on the DX coil model provided in the Modelica Buildings Library. Using multiple performance curves to represent the overall functionality of the heat pump, it is able to simulate the heat pump's total capacity and power usage under different operational modes (heating/cooling) and variable speed scenarios. The effectiveness of the proposed model is validated through a comparison between simulated values and measurements from a real heat pump testbed. The simulated capacity, EIR, and power correspond well with measurements for both heating and cooling conditions, demonstrating the model's capability in predicting variable-speed heat pump performance.

Future work in the following aspects can be considered:

- Improving Sensible Heat Ratio (SHR) Prediction: Although the current model performs well in predicting the total cooling capacity, the simulated sensible heat ratio does not align well with measurement values. SHR, which describes the ratio of sensible heat load to total heat load, needs further refinements to improve the model performance.
- Extending Application Scenarios: The proposed heat pump model can be applied to additional scenarios, such as building-to-grid systems or district heat pump systems (Yuhang Zhang et al. 2024). Further verification of its effectiveness in these contexts is needed.

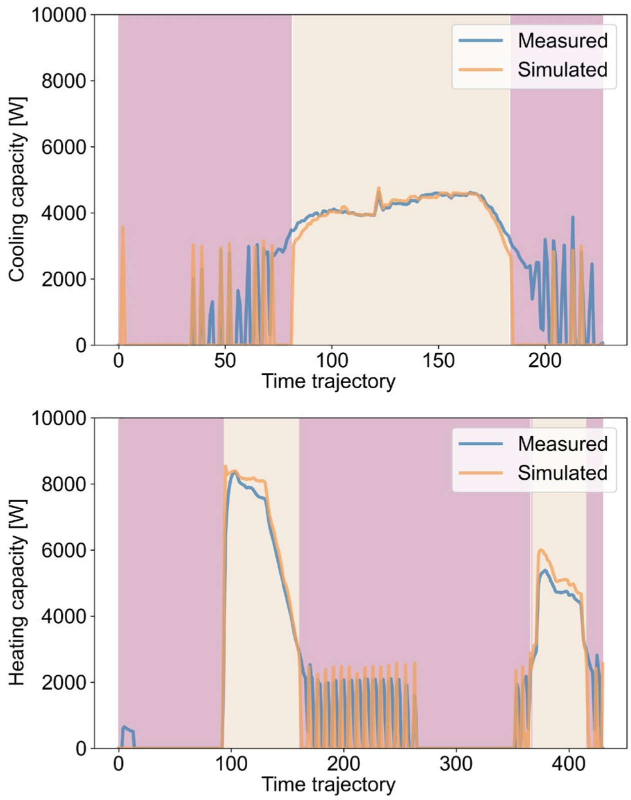

Figure 7. Comparisons between simulated and measured system capacity over two whole days (top: cooling, bottom: heating).

Acknowledgements

This work is partly supported by the National Science Foundation (2309030). The authors would also like to acknowledge the support and assistance provided by the manufacturer Trane.

References

Baccoli, Roberto, Costantino Mastino, and Giuseppe Rodriguez (2015). "Energy and Exergy Analysis of a Geothermal Heat Pump Air Conditioning System". In: *Applied Thermal Engineering* 86, pp. 333–347. DOI: 10.1016/j.applthermaleng.2015.03.046.

Calfa, Caleb et al. (2023). "Performance Assessment of a Real Water Source Heat Pump within a Hardware-in-the-Loop (HIL) Testing Environment". In: *Science and Technology for the Built Environment* 29.10, pp. 1011–1026. DOI: 10.1080/23744731.2023.2261810.

Chua, K. J., S. K. Chou, and W. M. Yang (2010). "Advances in Heat Pump Systems: A Review". In: *Applied Energy* 87.12, pp. 3611–3624. DOI: 10.1016/j.apenergy.2010.06.014.

Crawley, Drury B. et al. (2001). "EnergyPlus: Creating a New-Generation Building Energy Simulation Program". In: *Energy and Buildings*. Special Issue: BUILDING SIMULATION'99 33.4, pp. 319–331. DOI: 10.1016/S0378-7788(00)00114-6.

Fritzson, Peter and Vadim Engelson (1998). "Modelica — A Unified Object-Oriented Language for System Modeling and Simulation". In: *ECOOP'98 — Object-Oriented Programming*. Ed. by Eric Jul. Berlin, Heidelberg: Springer, pp. 67–90. ISBN: 978-3-540-69064-1. DOI: 10.1007/BFb0054087.

Gaur, Ankita Singh, Desta Z. Fitiwi, and John Curtis (2021). "Heat Pumps and Our Low-Carbon Future: A Comprehensive Review". In: *Energy Research & Social Science* 71, p. 101764. DOI: 10.1016/j.erss.2020.101764.

Huang, Shifang et al. (2019). "Performance Comparison of a Heating Tower Heat Pump and an Air-Source Heat Pump: A Comprehensive Modeling and Simulation Study". In: *Energy Conversion and Management* 180, pp. 1039–1054. DOI: 10.1016/j.enconman.2018.11.050.

Jorissen, Filip et al. (2018). "Implementation and verification of the IDEAS building energy simulation library". In: *Journal of Building Performance Simulation* 11.6, pp. 669–688.

Maier, Laura et al. (2024). "AixLib: an open-source Modelica library for compound building energy systems from component to district level with automated quality management". In: *Journal of Building Performance Simulation* 17.2, pp. 196–219.

Montagud, Carla, José Miguel Corberán, and Félix Ruiz-Calvo (2013). "Experimental and Modeling Analysis of a Ground Source Heat Pump System". In: *Applied Energy* 109, pp. 328–336. DOI: 10.1016/j.apenergy.2012.11.025.

Trane Technologies (2024a). *Ascend® Air-to-Water Heat Pump Model ACX*. https://www.trane.com/commercial/north-america/us/en/products-systems/chillers/air-cooled-chillers/ascend-air-to-water-heat-pump.html.

Trane Technologies (2024b). *Axiom™ Horizontal and Vertical Water Source Heat Pumps*. https://www.trane.com/commercial/north-america/us/en/products-systems/packaged-units-and-split-systems/water-source-heat-pumps/high-ef-horizontal-vertical-wshp.html.

Wetter, Michael et al. (2014). "Modelica Buildings Library". In: *Journal of Building Performance Simulation* 7.4, pp. 253–270. DOI: 10.1080/19401493.2013.765506.

Zhang, Ying et al. (2020). "Study on Model Uncertainty of Water Source Heat Pump and Impact on Decision Making". In: *Energy and Buildings* 216, p. 109950. DOI: 10.1016/j.enbuild.2020.109950.

Zhang, Yuhang et al. (2024). "Temperature Control Strategies for Fifth Generation District Heating and Cooling Systems: A Review and Case Study". In: *Applied Energy* 376, p. 124156. DOI: 10.1016/j.apenergy.2024.124156.

Zimmer, Dirk, Michael Meißner, and Niels Weber (2022). "The DLR ThermoFluid Stream Library". In: *Electronics* 11.22, p. 3790. DOI: 10.3390/electronics11223790.